Supplementary Information for Disentangling Heterogeneous Thermocatalytic Formic Acid Dehydrogenation from an Electrochemical Perspective

Xianxian Qin[1†], Jiejie Li[2†], Tianwen Jiang[1], Xian-Yin Ma[1], Kun Jiang[1,3], Bo Yang*[2], Shengli Chen[4], and Wen-Bin Cai*[1]

[1]Shanghai Key Laboratory of Molecular Catalysis and Innovative Materials, Collaborative Innovation Center of Chemistry for Energy Materials, Department of Chemistry, Fudan University, Shanghai, China.

[2]School of Physical Science and Technology, ShanghaiTech University, Shanghai, China.

[3]School of Mechanical Engineering, Shanghai Jiao Tong University, Shanghai, China.

[4]College of Chemistry and Molecular Sciences, Wuhan University, Wuhan, China.

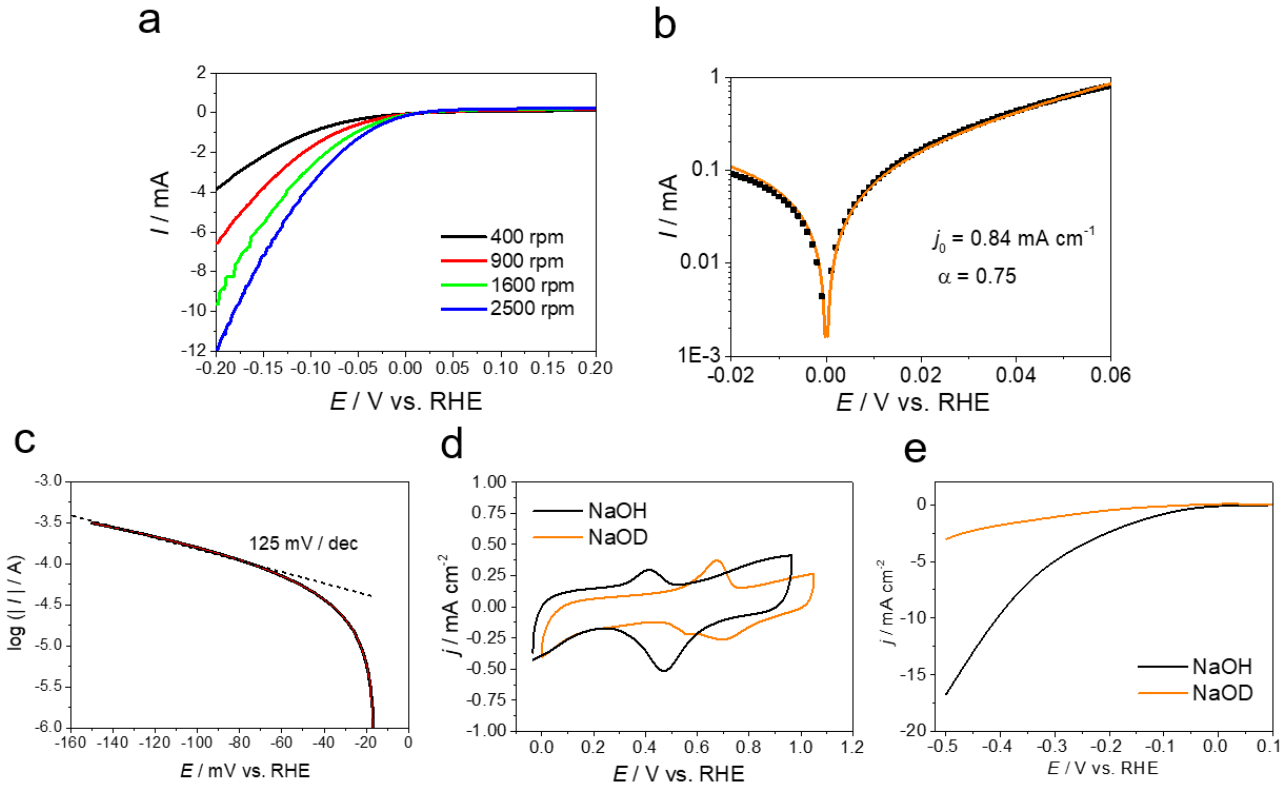

Supplementary Fig. 1 | Determination of RDS for HER on Pd/C. (a) Linear sweep voltammograms for Pd/C-covered RDE in a H_2-saturated 0.1 M $HClO_4$ solution (pH1) at different rotation rates with a scan rate of 10 mV/s. (b) Butler-Volmer equation fitting plot of HER/HOR kinetics on Pd/C-covered RDE in a H_2-saturated 0.1 M $HClO_4$ solution (pH1) at 1600 rpm. Black dots correspond to the experimentally determined by Koutecky Levich plot, and orange line corresponds to the Butler-Volmer equation fit line. (c) Tafel slope fitting of HER current against potential for Pd/C-covered RDE in an Ar-saturated 0.1 M LiOH solution (pH13) at 1600 rpm with a scan rate of 10 mV/s. (d) Cyclic voltammograms for Pd/C in an Ar-saturated 0.1 NaOH (or NaOD) in water (or heavy water) at pH13 with a scan rate of 50 mV/s. (e) Linear sweep voltammograms for Pd/C-covered RDE in an Ar-saturated NaOH (or NaOD) in water (or heavy water) at pH13 at 1600 rpm with a scan rate of 10 mV/s.

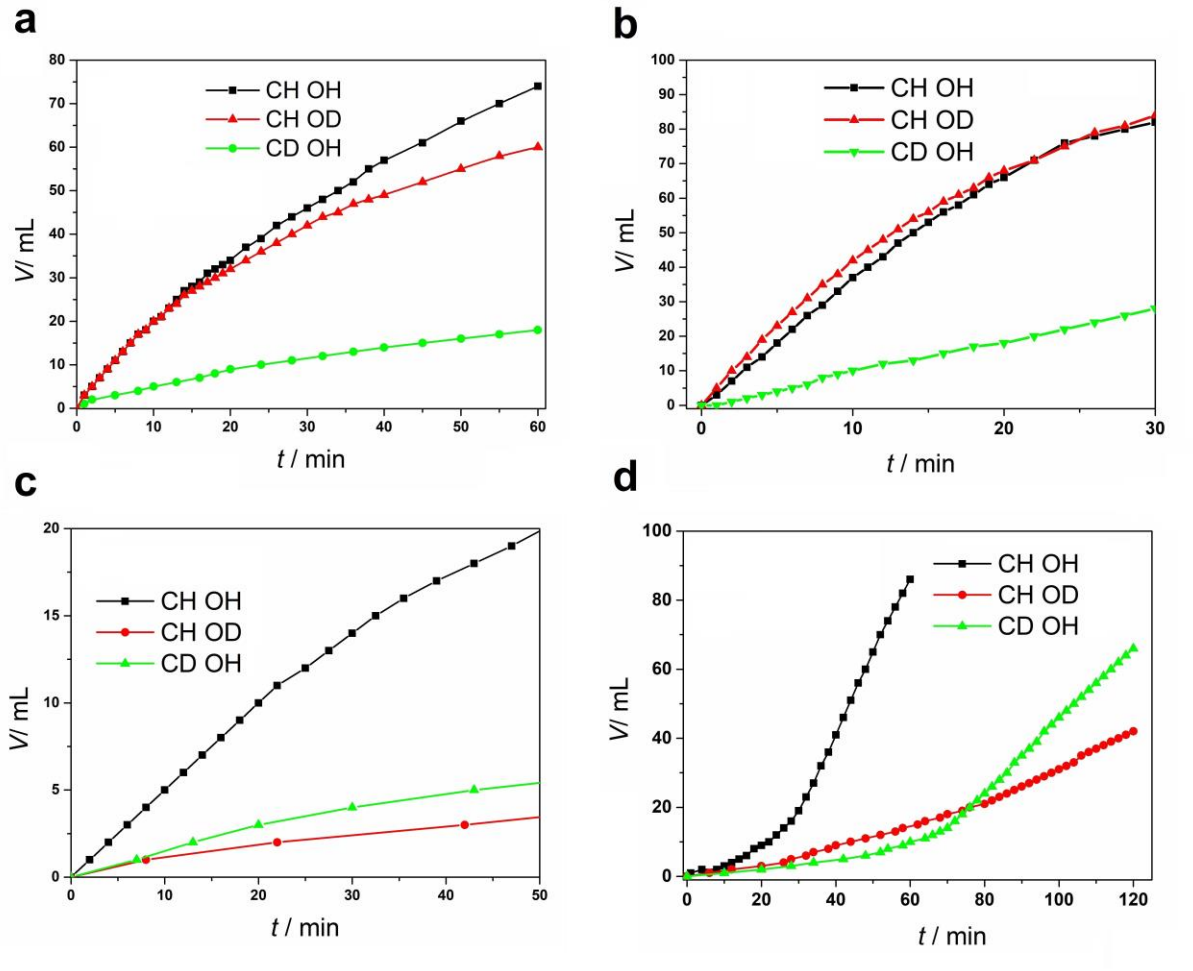

Supplementary Fig. 2 | KIE factor for FAD at varied pHs as determined from time course of gas evolution for FAD on Pd/C at (a) pH1 in 0.1 M $HClO_4$ + 1.0 M HCOOH; (b) pH3.7 in 0.2 M HCOOH + 0.2 M HCOONa; (c) pH~7 in 1.0 M HCOONa and (d) pH13 in 0.1 M KOH + 1.0 M HCOOK. Labels C-H(C-D) refer to (deuteride) formate/formic acid, and labels O-H(O-D) refer to (deuteride) water. Test condition: 298 K for pH 1, 3.7 and 7, and 333 K for pH 13.

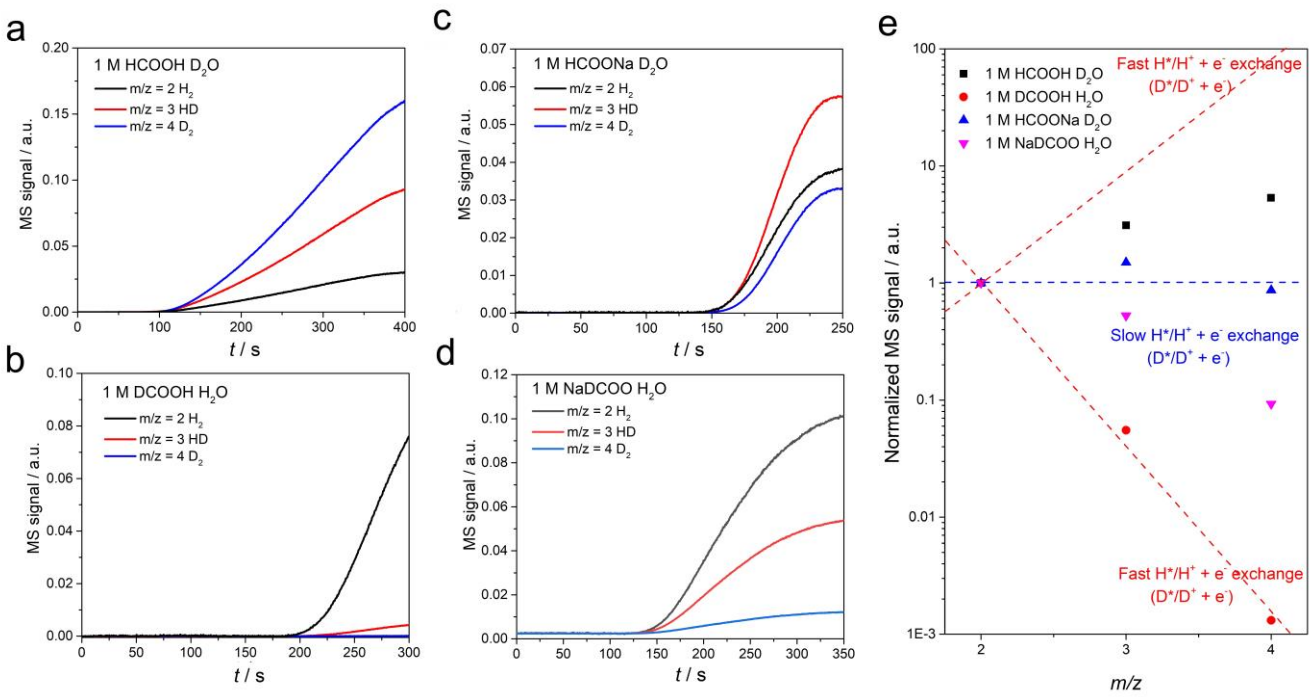

Supplementary Fig. 3 | Determination of the H origin of the product H_2 of FAD in acidic and neutral solutions by *in-situ* mass spectrometry in conjunction with isotope labelling. Time evolved mass signals of hydrogen gas evolution (H_2, HD and D_2) for FAD in 1 M HCOOH solution with heavy water (a), 1 M DCOOH solution with water (b), 1 M NaHCOO solution with heavy water (c) and 1 M NaDCOOH solution with water (d). a.u. stands for arbitrary units. (e) Plots of normalized abundances of H_2, HD and D_2 in the gas products during FAD as quantified by mass spectroscopy. Red dotted lines indicate the expected H_2/D_2 richness distribution when the inter-exchange $H^*+ D^+= H^+ + D^*$ due to $H^* = H^+ + e^-$ and $D^+ + e^- = D^*$ is fast and equilibrated, whereas blue dotted line indicates the expected H_2/D_2 richness distribution when the inter-exchange is slow and irreversible.

Isotope labelling tests for FAD at acidic and neutral solutions are measured by mass spectrometer to gain a deeper understanding in FAD mechanism. The product gases of FAD in different isotope labeled solutions are carried by Ar stream to the in-situ DMS (differential mass spectrometry) system to examine the isotope abundance. If the re-adsorption rate of H_2 (or HD, D_2) on Pd surface is low, which is guaranteed by quick transport of the gas product away from the reaction system and fast response of in-situ DMS, the isotope abundance distribution in the gas product is useful for mechanism analysis.

Based on the reaction mechanism models given in Fig. 1a and Fig. 2g, the isotopic richness distribution of H_2, HD and D_2 in the gas product is direct correlated to the surface coverage of H* and D*.

$$r_{H_2} = k_{H_2}\theta_{H*}^2$$

$$r_{D_2} = k_{D_2}\theta_{D*}^2$$

$$r_{HD} = 2k_{HD}\theta_{H*}\theta_{D*}$$

$$r_{H_2}: r_{D_2}: r_{HD} = k_{H_2}\theta_{H*}^2: k_{D_2}\theta_{D*}^2: 2k_{HD}\theta_{H*}\theta_{D*} = \theta_{H*}^2: \frac{k_{D_2}}{k_{H_2}}\theta_{D*}^2: 2\frac{k_{HD}}{k_{H_2}}\theta_{H*}\theta_{D*}$$

In consideration that H recombination step is a bond-making step, the KIE factors $\frac{k_{D_2}}{k_{H_2}}$ and $\frac{k_{HD}}{k_{H_2}}$ are expected to be close to 1, which yields,

$$r_{H_2}: r_{D_2}: r_{HD} = \theta_{H*}^2: \theta_{D*}^2: 2\theta_{H*}\theta_{D*}$$

The reactant reagents used here are 1 M HCOOH in D_2O, 1 M DCOOH in H_2O, 1 M HCOONa in D_2O and 1 M DCOONa in H_2O, in which the H atoms from either C-H or O-H is substituted by D atoms. Therefore, in an ideal situation where both C-H(D) cleavage and O-H(D) cleavage to form surface H*(D*) are kinetically slow and irreversible, formation of a surface H* is always followed by a D* to keep the catalytic cycle complete, that is,

$$\theta_{H*}: \theta_{D*} = 1:1$$

The isotopic distribution in the gas is expected to be,

$$r_{H_2}: r_{D_2}: r_{HD} = 1: 1: 2$$

This scenario was emerged in the case of FAD in the neutral solution of 1 M HCOONa in D_2O. (See Supplementary Fig. 3c)

On the other hand, in acidic solution, we have known that electrochemical adsorption/desorption is fast and reversible thus in equilibrium. Therefore, the surface H* and D* can be readily exchanged with the protonic H^+ in the water (or D^+ in the heavy water). Noted that the concentration of (heavy) water is 55.5 mol/L which is a large reservoir for proton species. Therefore, in a (heavy) water solution, H* (D*) will prevail on the Pd surface,

$$\theta_{H*} > \theta_{D*}$$

$$(\theta_{H*} < \theta_{D*})$$

The isotopic distribution in the gas product is expected to be,

$$r_{H_2} \gg r_{D_2}$$

$$(r_{H_2} \ll r_{D_2})$$

which was shown in the case of FAD in the acidic solution, especially in the case of 1 M DCOOH in H_2O. (See Supplementary Fig. 3b)

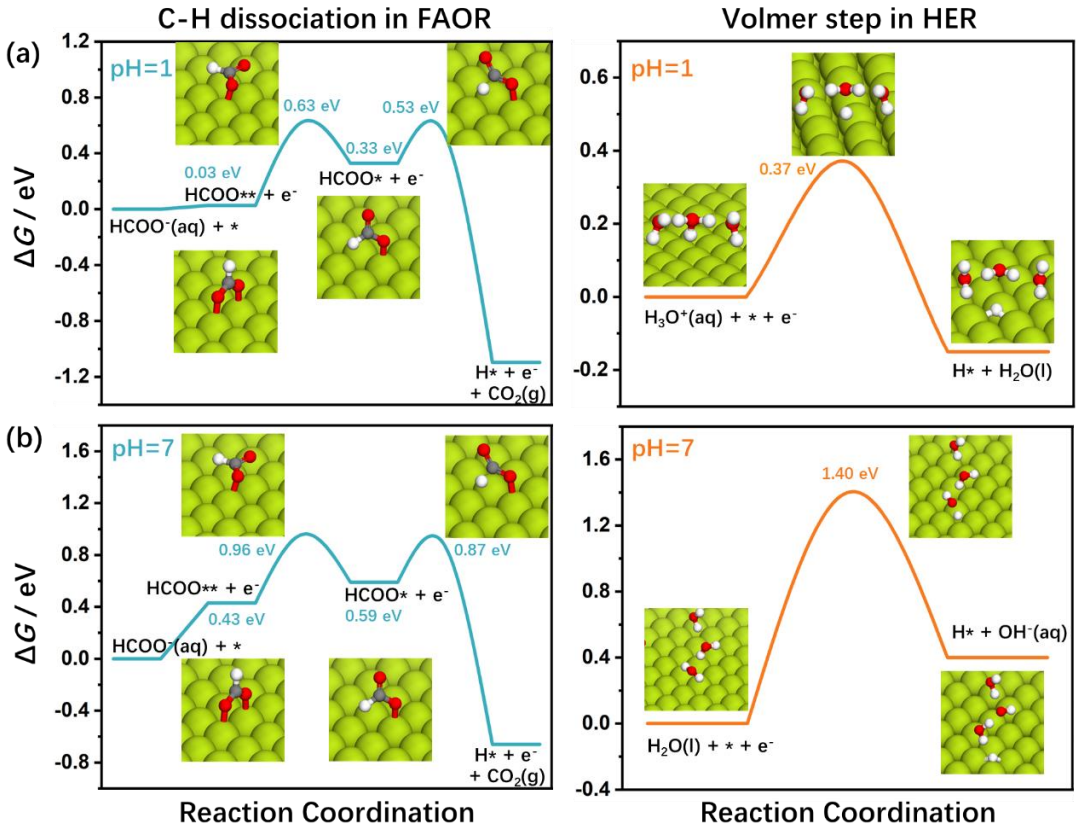

Supplementary Fig. 4 | Free-energy profiles for C-H dissociation and Volmer step under 0 V (vs. RHE) at pH1 and pH7 over clean Pd(111) surface.

Two main roles of the local water are generally considered during catalytic processes. The first one is simply the solvation effect, which suggests that local water can help stabilize hydrogen ion, formic acid and formate intermediate with hydrogen bonding. Here, we involved implicit solvation model throughout the simulations, which can provide relatively accurate elaboration for solvent-species interactions. For the solvation effect of hydrogen ion, explicit water molecules were also included in the models.

The other effect is that the local water may participate in chemical reactions and affect the reaction barriers. According to the work of Qi et al.,[1] the local water dramatically accelerates the O-H dissociation in formic acid decomposition over Pt(111), but the C-H dissociation barrier is less sensitive as the local water only show stabilization effects. Without considering the presence of water, the C-H dissociation barrier is 0.50 eV, but the addition of explicit water molecules only reduces the barrier to 0.26 eV.[1] Although the results were obtained over Pt(111), we believe the trend is also valid over Pd(111). Given that the implicit solvation model was considered in our work, the difference between the barriers determined in our model and those in the presence of explicit water molecules should be even smaller, which would not alter our conclusions regarding the identification of rate determining step between FAOR / HER.

.

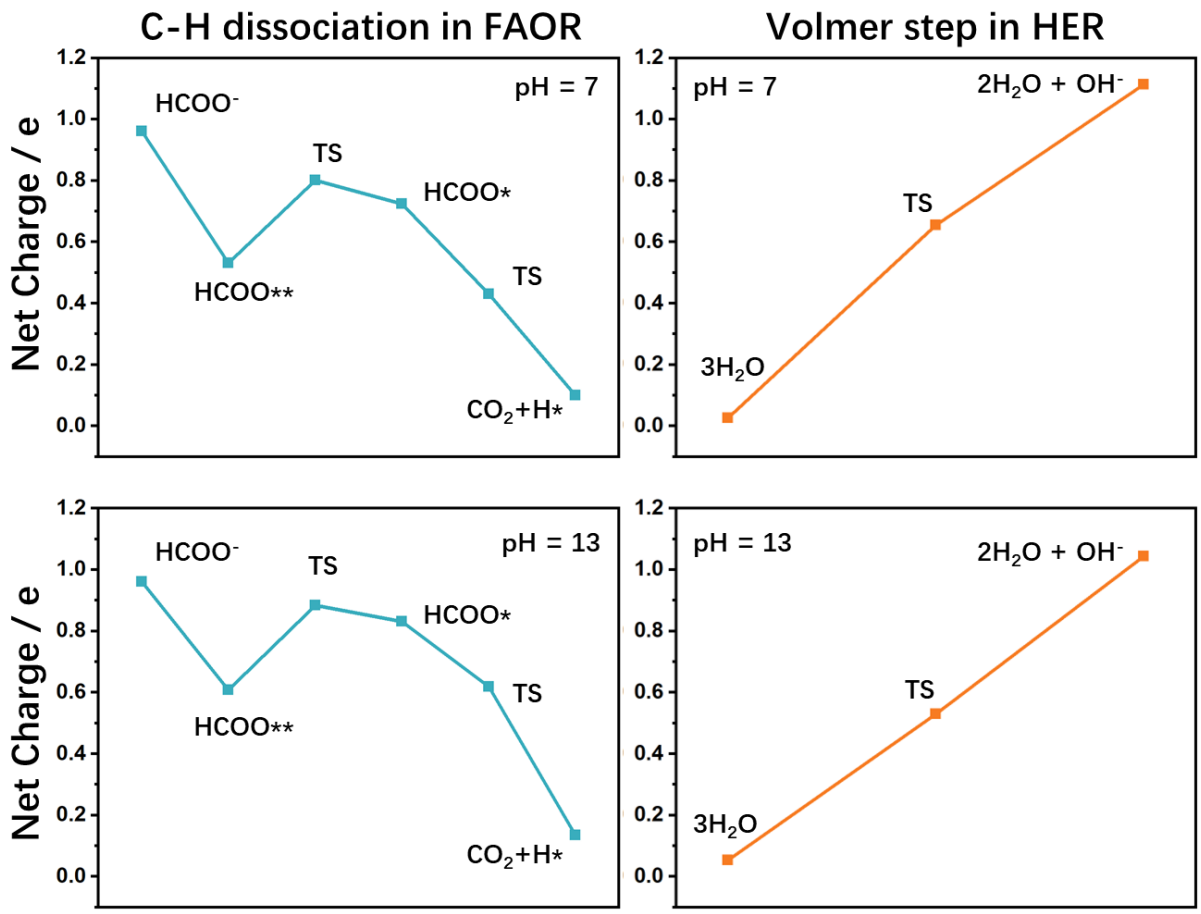

Supplementary Fig. 5 | Net charge analysis for FAOR and HER intermediates. Net charge changes of reaction species during C-H dissociation in formic acid oxidation and Volmer process in hydrogen evolution under 0 V (vs. RHE) at pH7 and pH13.

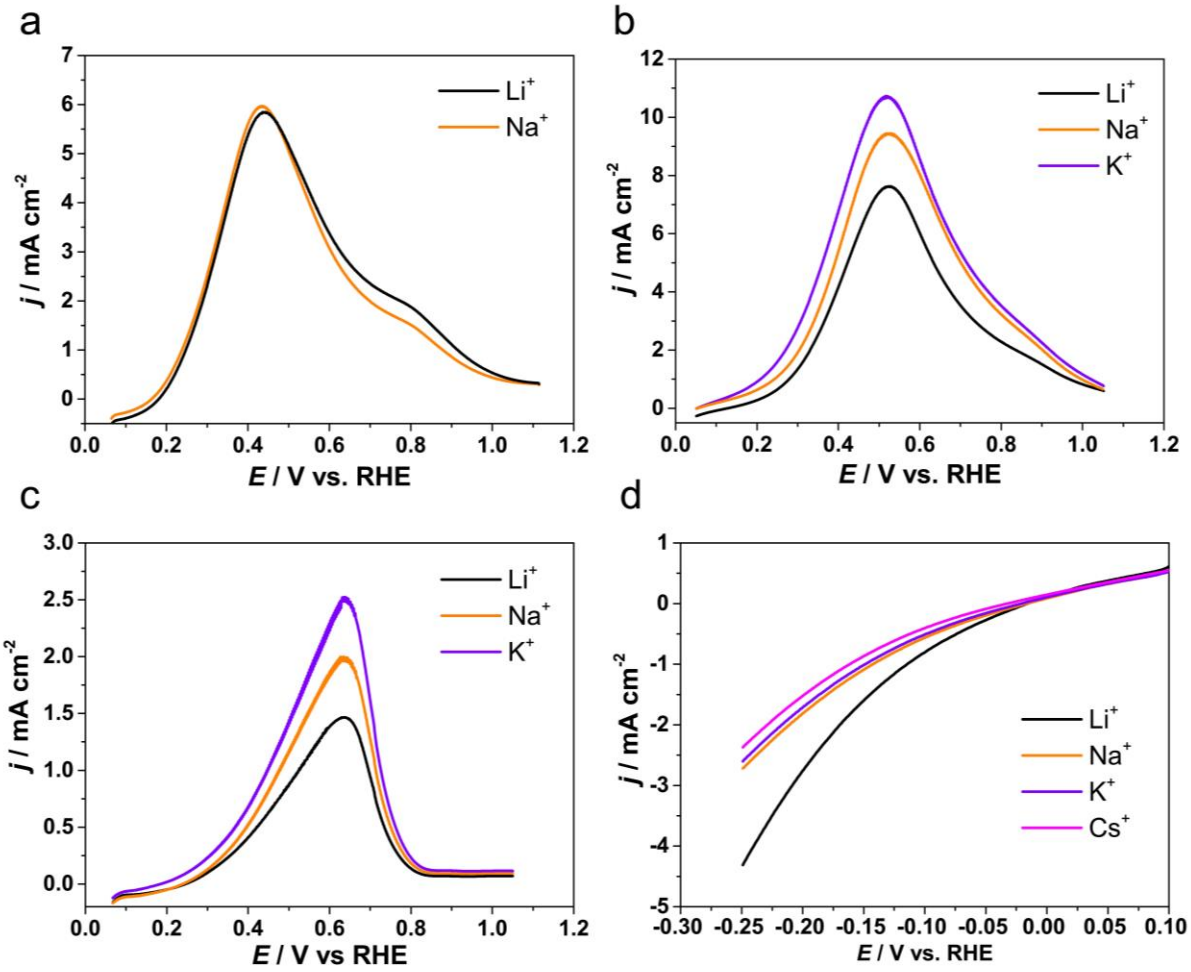

Supplementary Fig. 6 | Cation effect measurements for FAOR and HER on Pd/C catalyst. Linear sweep voltammograms from 0.05 to 1.10 V vs. RHE at 10 mV/s in solutions containing (a) 0.1 M HCOOH +0.1 M $HClO_4$ +0.1 M ClO_4^- (pH1), (b) 0.1 M HCOOH + 0.1 M $HCOO^-$ + 0.1 M SO_4^{2-} (pH3.7) and (c) 0.1 M $HCOO^-$ + 0.1 M OH^- (pH13) with different cation entities, the RDE is set at 1600 rpm. (d) Linear sweep voltammograms from 0.10 to -0.25 V vs. RHE at 2 mV/s in H_2 -saturated 0.1 M OH^- (pH13) with different metal cations, the RDE is set at 1600 rpm.

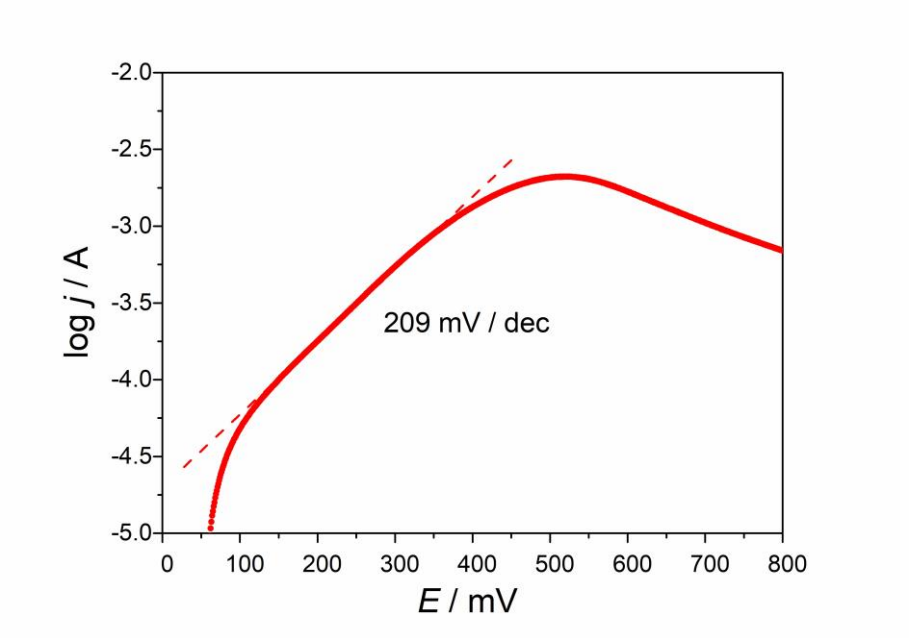

Supplementary Fig.7 | Tafel slope analysis for FAOR on Pd/C at pH 3.7. Tafel slope fitting of FAOR current against potential on Pd/C in 0.1 M HCOOH + 0.1 M HCOOK + 0.1 M K_2SO_4 solution at pH 3.7, original data are adapted from **Supplementary Fig. 6b**.

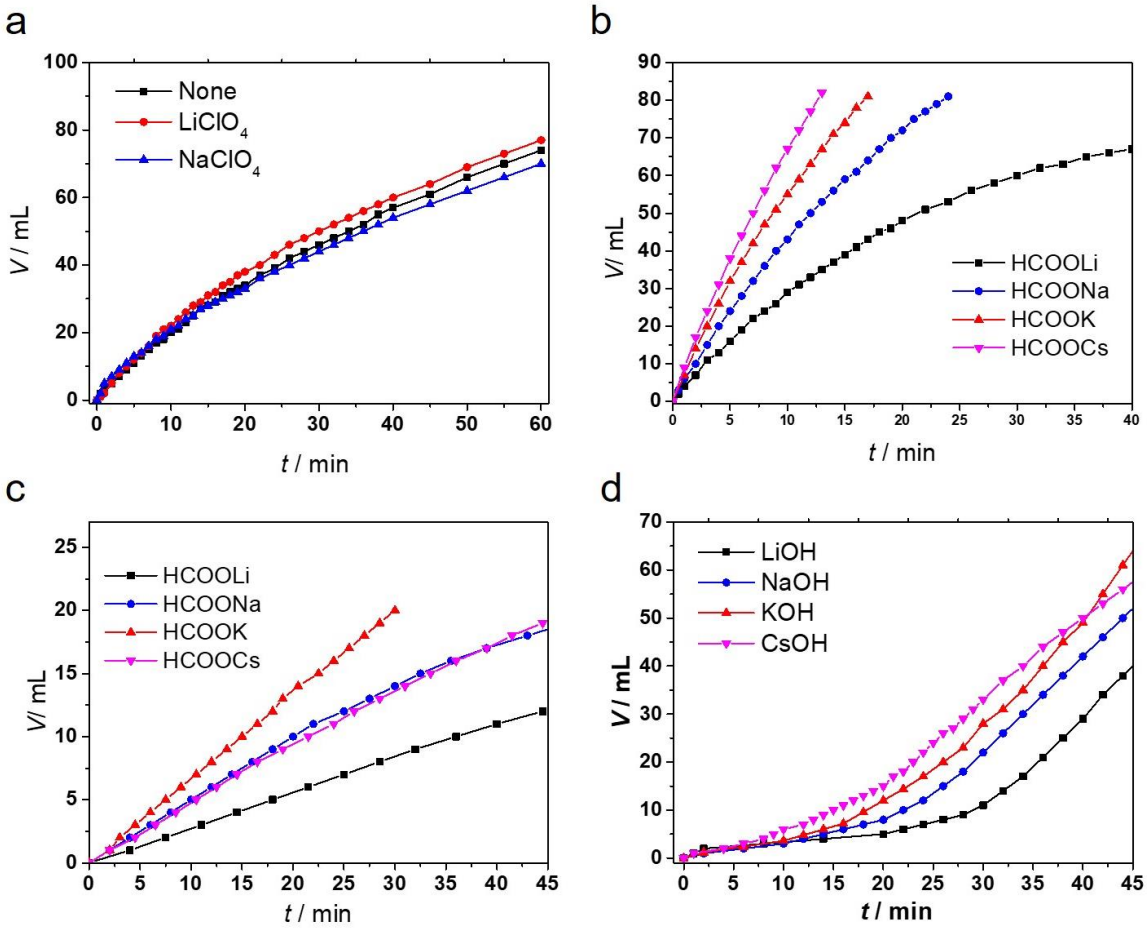

Supplementary Fig. 8 | Time course of gas evolution for FAD on Pd/C with cation effect at varied pH. Time course of gas evolution for FAD on Pd/C (a) at pH1, (b) pH3.7, (c) pH~7 and (d) pH13. Solutions: 0.1 M $HClO_4$ + 1.0 M HCOOH + 0.1 M $MClO_4$ (label None refers to 0.1 M $HClO_4$ + 1.0 M HCOOH without adding metal cations M^+) at pH1, 0.2 M HCOOH + 0.2 M HCOOM at pH3.7, 1.0 M HCOOM at pH~7, and 0.1 M MOH + 1.0 M HCOOM at pH13. Test condition: 298 K for pH1, 3.7 and 7, 333 K for pH13.

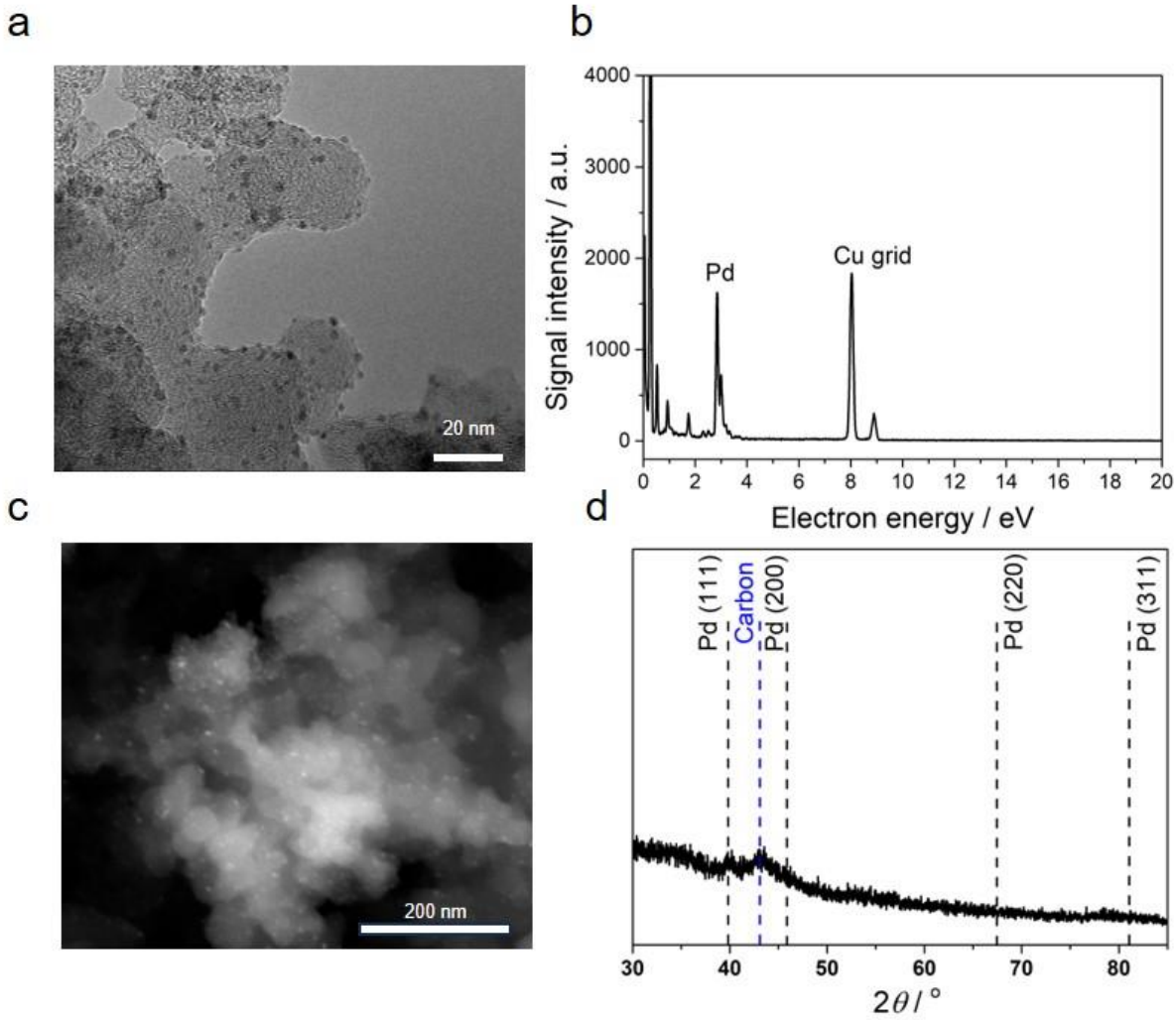

Supplementary Fig. 9 | Physical Characterizations of the as-prepared 5 wt.% Pd/C catalyst. (a) HR-TEM characterization of the as-prepared Pd/C catalyst. (b) EDS spectrum of the as-prepared Pd/C catalyst. a.u. stands for arbitrary units. (c) HR-SEM characterization of the as-prepared Pd/C catalyst. (d) XRD characterization of the as-prepared Pd/C catalyst.

The TEM, SEM and XRD characterizations of the 5 wt.% Pd/C catalyst used in this work show Pd nanoparticles with an average size of 2.3 nm are well dispersed on Vulcan XC72 carbon black support.

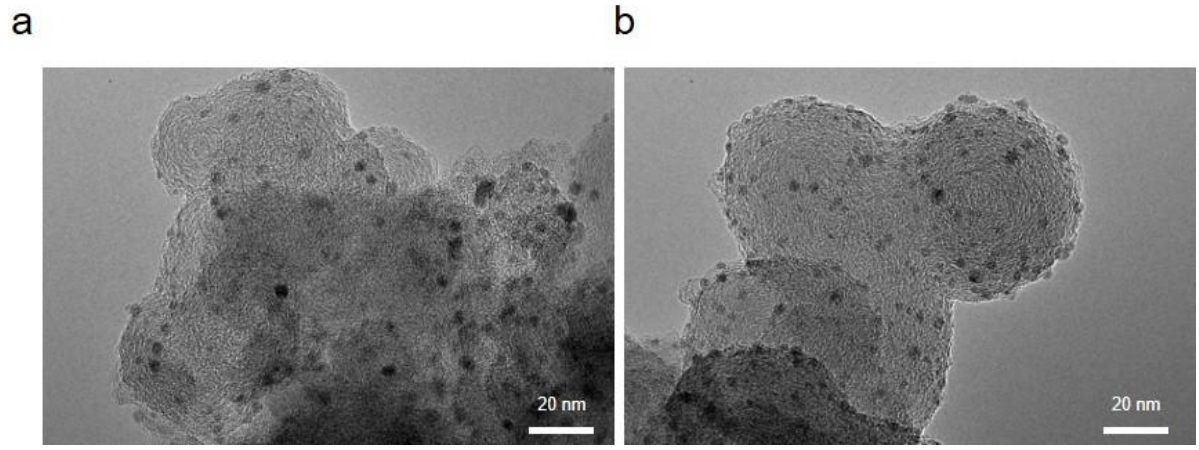

Supplementary Fig. 10 | Physical Characterizations of the used Pd/C catalyst after electrochemical reactions. (a) HR-TEM image of the Pd/C catalyst after FAOR test, or (b) after HER test at 323 K. Relevant electrochemical results are shown in Fig. 7c.

After electrochemical measurements as described in Fig. 7c, the mean particle size of Pd nanoparticles on carbon black grows slightly from ~2.3 nm to ~2.6 nm as statistically estimated by TEM images in **Supplementary Figs. 10a** and **10b**.

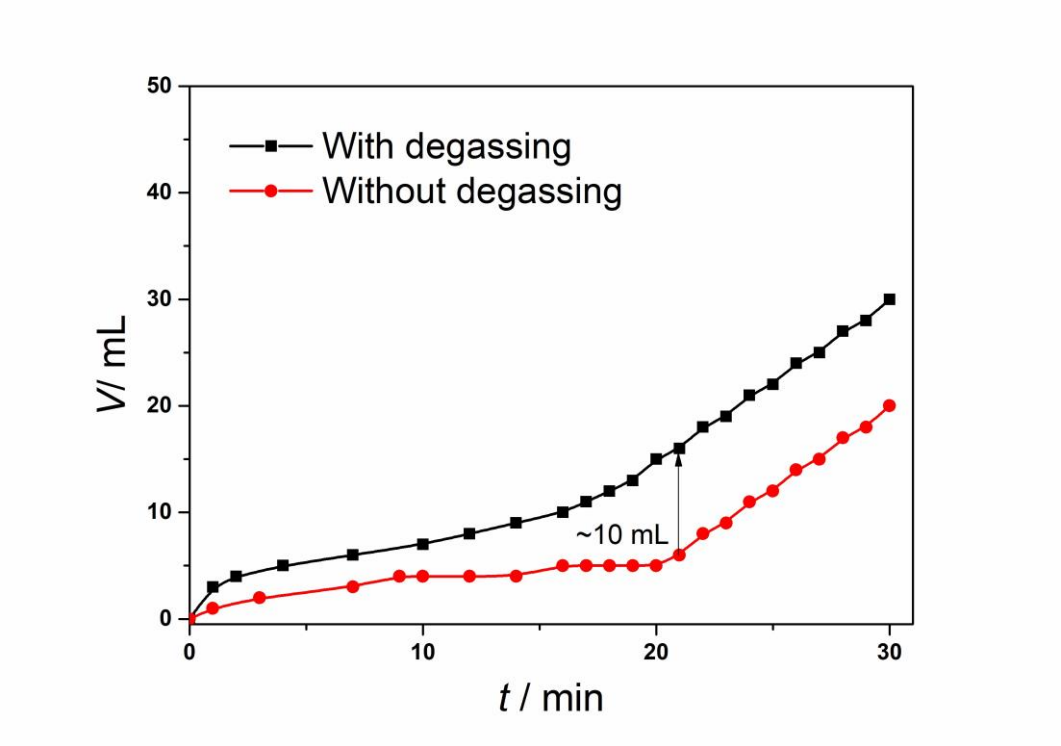

Supplementary Fig. 11 | Influence of oxygen residue in the reaction system on FAD at pH13. Time course of gas evolution for FAD in 0.1 M KOH + 1.0 M HCOOK solution at 333 K with/without deaeration procedure in a 25 mL flask.

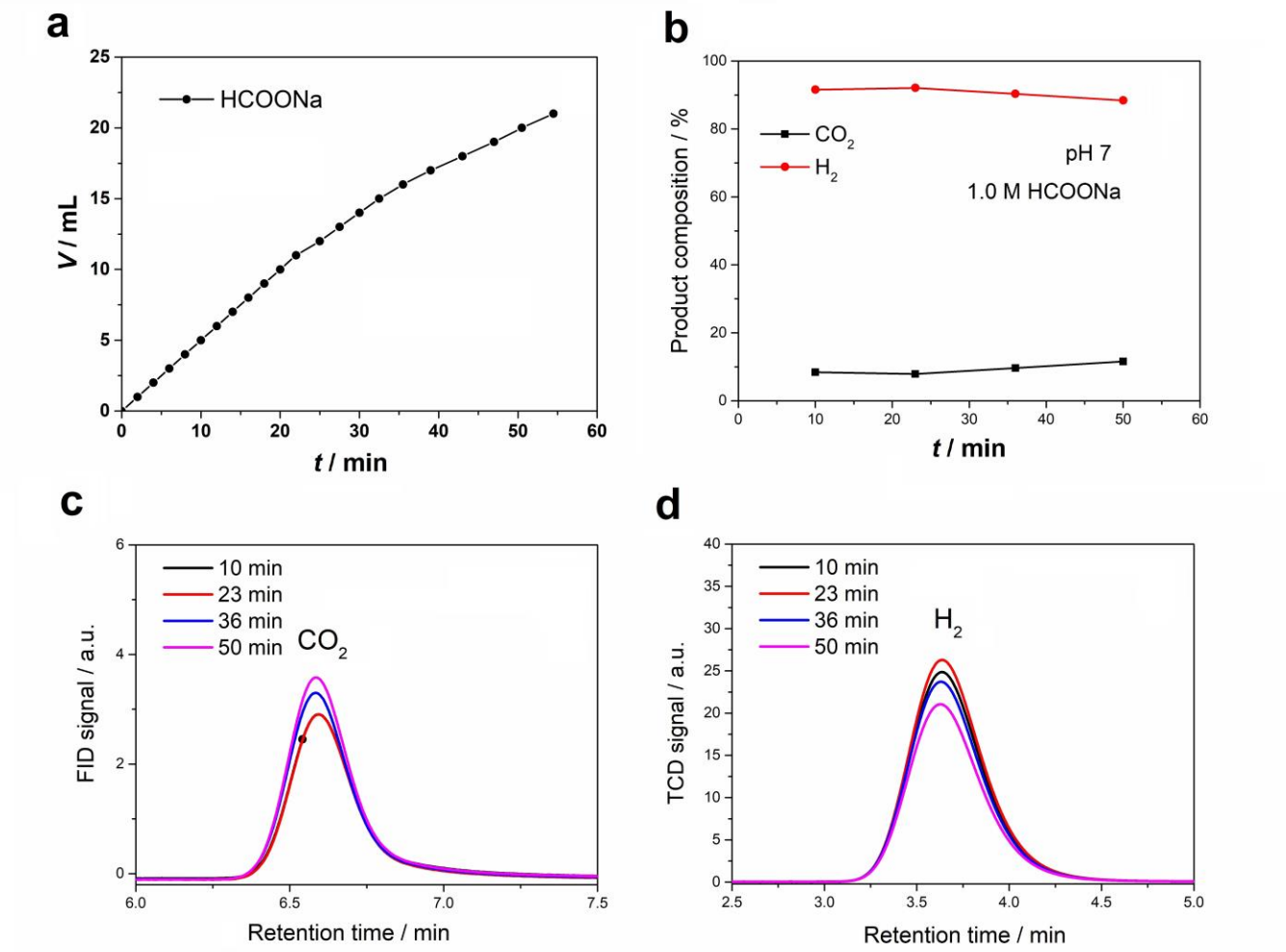

Supplementary Fig. 12 | Product analysis of FAD on Pd/C at pH~7 by GC. (a) Time course of gas evolution for FAD in 1.0 M HCOONa solution (pH~7) at 298 K. (b) The plots of collectable gas composition against reaction time measured by GC. (c) The GC signal peaks of CO_2 against reaction time measured by FID detector of GC. (d) The GC signal peaks of H_2 against reaction time measured by TCD detector of GC. a.u. stands for arbitrary units.

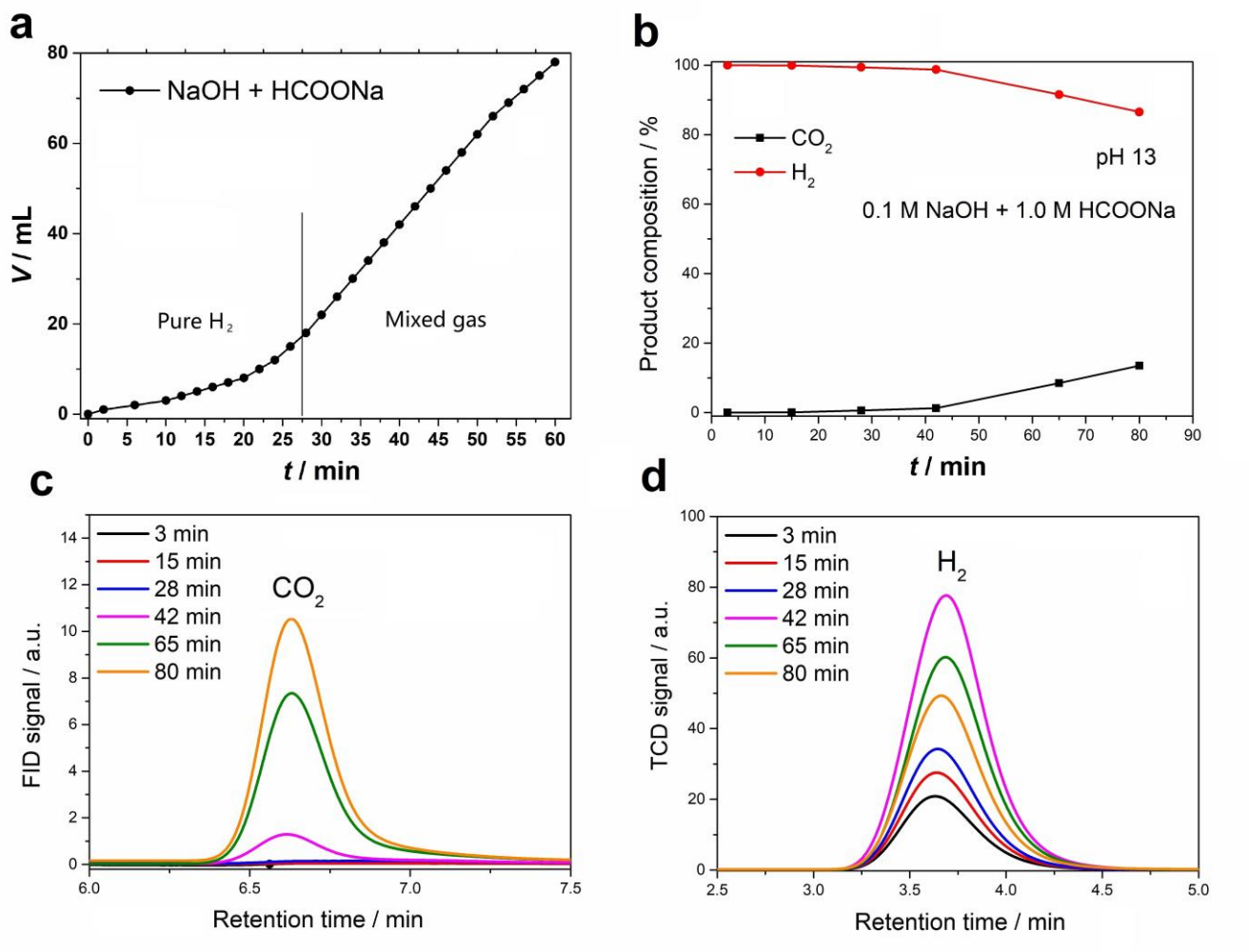

Supplementary Fig. 13 | Product analysis of FAD at pH13 by GC. (a) Time course of gas evolution for FAD reaction in 0.1 M NaOH + 1.0 M HCOONa (pH13) solution at 333 K. (b) The plots of collectable gas composition against reaction time measured by GC. (c) The GC signal peaks of CO_2 against reaction time measured by FID detector of GC. (d) The GC signal peaks of H_2 against reaction time measured by TCD detector of GC. a.u. stands for arbitrary units.

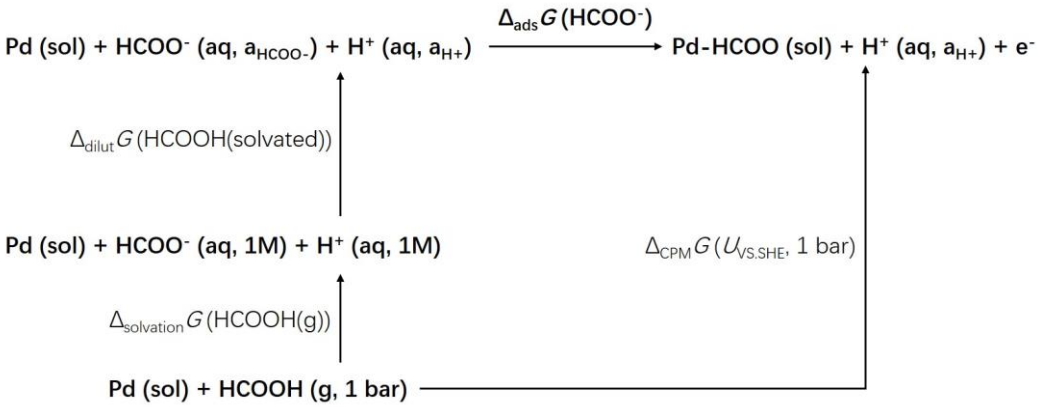

Supplementary Figure 14. Thermodynamic cycle used to calculate adsorption free energy of formate anion from solution.

Supplementary Table 1 | Reagents for FAD tests in KIE measurements and cation effect measurements

KIE measurement	pH1	0.1 M $HClO_4$ + 1.0 M HCOOH + H_2O
		0.1 M $HClO_4$ + 1.0 M DCOOH + H_2O
		0.1 M $HClO_4$ + 1.0 M HCOOH + D_2O
	pH3.7	0.2 M HCOOH + 0.2 M HCOONa + H_2O
		0.2 M DCOOH + 0.2 M DCOONa + H_2O
		0.2 M HCOOH + 0.2 M HCOONa + D_2O
	pH~7	1.0 M HCOONa + H_2O
		1.0 M DCOONa + H_2O
		1.0 M HCOONa + D_2O
	pH13	0.1 M KOH + 1.0 M HCOOK + H_2O
		0.1 M KOH + 1.0 M DCOOK + H_2O
		0.1 M KOH + 1.0 M HCOOK + D_2O
Cation effect measurement	pH1	0.1 M $HClO_4$ + 1.0 M HCOOH
		0.1 M $HClO_4$ + 1.0 M HCOOH + 1.0 M $LiClO_4$
		0.1 M $HClO_4$ + 1.0 M HCOOH + 1.0 M $NaClO_4$
	pH3.7	0.2 M HCOOH + 0.2 M HCOOLi
		0.2 M HCOOH + 0.2 M HCOONa
		0.2 M HCOOH + 0.2 M HCOOK
		0.2 M HCOOH + 0.2 M HCOOCs
		0.2 M HCOOH + 0.2 M $HCOONH_4$
	pH~7	1.0 M HCOOLi
		1.0 M HCOONa
		1.0 M HCOOK
		1.0 M HCOOCs
		1.0 M $HCOONH_4$
	pH13	0.1 M LiOH + 1.0 M HCOOLi
		0.1 M NaOH + 1.0 M HCOONa
		0.1 M KOH + 1.0 M HCOOK
		0.1 M CsOH + 1.0 M HCOOCs

Supplementary Table 2 | Reagents for FAOR tests in KIE measurements and cation effect measurements

KIE measurement	pH1	0.1 M $HClO_4$ + 0.1 M HCOOH + H_2O
		0.1 M $HClO_4$ + 0.1 M DCOOH + H_2O
		0.1 M $HClO_4$ + 0.1 M HCOOH + D_2O
	pH3.7	0.2 M HCOOH + 0.2 M HCOONa + 0.2 M $NaClO_4$ + H_2O
		0.2 M DCOOH + 0.2 M DCOONa + 0.2 M $NaClO_4$ + H_2O
		0.2 M HCOOH + 0.2 M HCOONa + 0.2 M $NaClO_4$ + D_2O
	pH13	0.1 M NaOH + 0.1 M HCOONa + H_2O
		0.1 M NaOH + 0.1 M DCOONa + H_2O
		0.1 M NaOH + 0.1 M HCOONa + D_2O
Cation effect measurement	pH1	0.1 M $HClO_4$ + 0.1 M HCOOH + 0.1 M $LiClO_4$
		0.1 M $HClO_4$ + 0.1 M HCOOH + 0.1 M $NaClO_4$
	pH3.7	0.1 M HCOOH + 0.1 M HCOOLi + 0.1 M Li_2SO_4
		0.1 M HCOOH + 0.1 M HCOONa + 0.1 M Na_2SO_4
		0.1 M HCOOH + 0.1 M HCOOK + 0.1 M K_2SO_4
	pH13	0.1 M LiOH + 0.1 M HCOOLi
		0.1 M NaOH + 0.1 M HCOONa
		0.1 M KOH + 0.1 M HCOOK

Supplementary Note 1 Detailed procedures for electrochemical tests

Electrochemical measurements for FAOR. Before each measurement, Ar was bubbled into the solution to remove the dissolved oxygen for over 15 min. Afterwards, the pre-cleaned Pd/C electrode was transferred in the newly deaerated electrolyte with cyclic voltammetry run between OCP and 1.05 V vs. RHE. The scan rate was controlled at 10 mV/s and the RDE rotating rate was set at 1600 rpm. In alkaline solutions a commercial Hg/HgO electrode served as the reference electrode, while in acidic solutions a home-made RHE served as the reference electrode.

Electrochemical measurements for HER/HOR. The cell designed for HER/HOR test was a five-neck cell, the extra two necks were used for the inlet and outlet of H_2 stream. Throughout the experiment, the ambient pressure H_2 stream was bubbled in the solution at a rate of ~ 75 sccm. Linear sweep voltammograms for the Pd/C-covered RDE were recorded sequentially at 2 mV/s with 400, 900, 1600 and 2500 rpm. A homemade RHE and a commercial Hg/HgO electrode served as the reference electrode in acidic and alkaline solutions, respectively, and a Pt mesh served as the counter electrode.

Open circuit potential (OCP) measurement for FAD. Before each measurement, Ar was bubbled into the solution to remove the oxygen residues in a formic acid-formate solution for over 15 min. And the Ar gas was continuously flowing at the headspace of the solution during the OCP measurement to diminish the interference of O_2 from air. The OCP of the Pd/C film electrode was recorded in a static solution for 20 min against a commercial Hg/Hg_2SO_4 (Hg/HgO) reference electrode in acidic (alkaline) solutions, respectively. The OCP dip (the lowest value) during the 20-min long test was considered as the steady state OCP for FAD. Three parallel measurements were conducted for each solution.

Supplementary Note 2 Adsorption Free energy calculations

A thermodynamic cycle reported by Hansen et al.[2] was used to calculate the adsorption free energy of formate anion from solution onto electrode surface, the results of which are shown in **Supplementary Figure 11.**

The equation used is

$\Delta G_{ads}(HCOO^-) = \Delta G_{CPM}(U_{vs.\ SHE}) - \Delta G_{solvation}(HCOOH(g)) - \Delta G_{dilut}(HCOOH(solvated))$

Each term in the righthand side of the equation can be calculated as follows.

$\Delta G_{CPM}(U_{vs.\ SHE})$ is the adsorption energy calculated by constant potential method as:

$\Delta G_{CPM}(U_{vs.\ SHE}) = G_{HCOO*}(U) + G_{H^+} - G_{HCOOH+*}(U)$

where $G_{HCOO*}(U)$ and $G_{HCOOH+*}(U)$ are the grand canonical free energy, and G_{H^+} is the free energy of proton.

$\Delta G_{solvation}(HCOOH(g))$ is the free energy of solvation, and equals to the difference between the standard formation Gibbs energy of gaseous formic acid (-350.83 kJ mol^{-1}) and formate anion (-351.00 kJ mol^{-1}), considering that the standard formation Gibbs energy of H^+ is 0.[3]

The free energy of dilution $\Delta G_{dilut}(HCOOH(solvated))$ was calculated as:

$\Delta G_{dilut}(HCOOH(solvated)) = RT\ln(a_{H^+}a_{HCOO^-}) = -0.0592pH$

Considering the 1M concentration of formate in KIE experiment, we approximate a_{HCOO^-} to be 1M for convenience here.

To convert the DFT energies into Gibbs free energies at 298.15 K, entropy corrections for gas molecule and liquid water molecules were considered, which can be obtained from NIST database.[3] Entropy corrections used for gaseous H_2, gaseous formic acid and gaseous CO_2 was -0.40 eV, -0.77 eV and -0.66 eV, respectively. For H_2O, entropy correction of liquid phase was -0.22 eV.

Supplementary Note 3. Calculation details for the GCP-K method.

The Grand Canonical Potential Kinetics (GCP-K) method developed by Goddard III's group[4-6] was used to predict the reaction free energies and activation free energies at target electrode potentials. GCP-K uses a Legendre transformation to convert fixed charge free energy, F(n) (equation S1), to grand canonical free energy, GCP(U) (equation S2), allowing the free energy for heterogeneous electrochemical reactions to depend on the applied potential (U).

$$F(n) = -\frac{1}{2C_{diff}}(n - n_0)^2 + (\mu_{e,SHE} - eU_{PZC})(n - n_0) + F_0 \qquad (S1)$$

$$GCP(U) = \frac{e^2 C_{diff}}{2}(U - U_{PZC})^2 + n_0 eU + F_0 - n_0 \mu_{e,SHE} \qquad (S2)$$

where n_0 is the number of electrons at zero net charge, C_{diff} is the differential capacitance, U_{PZC} is the potential of zero charge, and F_0 is $F(n = n_0)$.

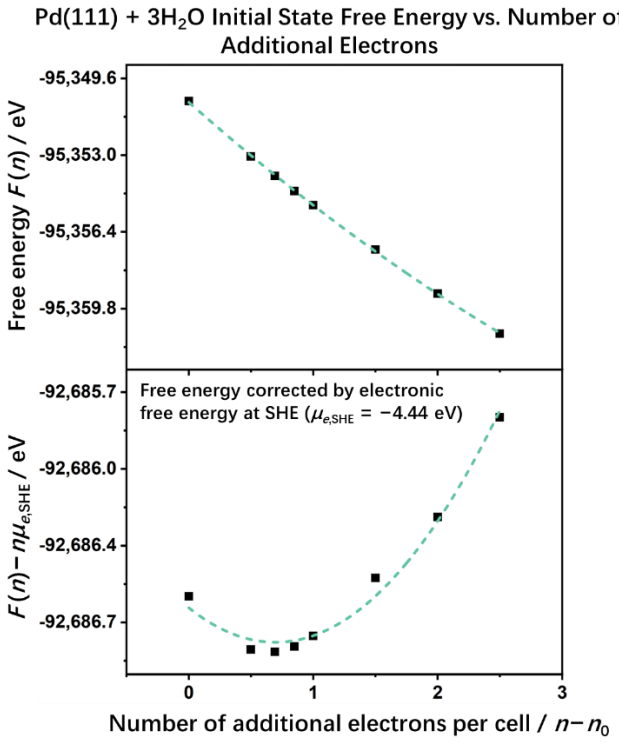

Supplementary Figure 15. Free energy as a function of the number of additional electrons ($n - n_0$) for the Pd(111) + $3H_2O$ initial state, before (above) and after (bottom) correcting the free energy contribution of electrons at SHE. The points are energies calculated using DFT and dashed curves are quadratic fittings. The quadratic nature of the free energy dependence on the number of electrons n is more apparent after correcting the free energy contribution of electrons (bottom).

Supplementary Table 3 | Parameters obtained from quadratic fitting to obtain the F(n) and GCP(U) for the Pd(111) system.

Species	$\frac{1}{2C_{diff}}$ (eV/electron^2)	$(\mu_{e,SHE} - eU_{PZC})$ (eV/electron)	F_0 (eV)	n_0
*+3H_2O_IS	0.49	−5.06	−95350.66	600
*+2H_2O+H-OH_TS	0.34	−4.92	−95349.44	600
2H_2O+H*_FS	0.70	−6.56	−95348.67	600
*+2H_2O+H_3O^+_IS	0.60	−4.75	−95367.90	601
*+2H_2O+H_2O-H_TS	0.43	−5.04	−95367.33	601
3H_2O+H*_FS	0.62	−5.29	−95367.57	601
HCOOH+*	0.36	−4.91	−95002.54	594
$HCOO_B$	0.42	−4.95	−94986.97	593
$HCOO_B \rightarrow_M$_TS	0.42	−5.09	−94986.26	593
$HCOO_M$	0.41	−5.17	−94986.52	593
H-COO_M_TS	0.45	−5.15	−94986.34	593
H*+CO_2	0.57	−5.14	−94987.38	593

Supplementary Table 4 | Parameters obtained from quadratic fitting to obtain the GCP(U) for Pd(111) with 0.44 ML of surface hydrogen system.

Species	$\frac{1}{2C_{diff}}$ (eV/electron^2)	$(\mu_{e,SHE} - eU_{PZC})$ (eV/electron)	F_0 (eV)	n_0
$3H_2O$_IS	0.25	−4.56	−95417.18	604
$2H_2O$+H-OH_TS	0.35	−5.05	−95415.51	604
$2H_2O$+H*_FS	0.63	−6.26	−95415.05	604
HCOOH+*	0.38	−4.90	−95068.91	598
$HCOO_B$	0.22	−4.56	−95053.36	597
$HCOO_B \rightarrow_M$_TS	0.24	−4.70	−95052.74	597
$HCOO_M$	0.32	−4.94	−95052.84	597
H-COO_M_TS	0.26	−4.66	−95052.80	597
H*+CO_2	0.27	−4.60	−95053.77	597

Supplementary Table 5 | Parameters obtained from quadratic fitting to obtain the GCP(U) for Pd(111) with 0.66 ML of surface hydrogen system.

Species	$\frac{1}{2C_{diff}}$ (eV/electron^2)	$(\mu_{e,SHE} - eU_{PZC})$ (eV/electron)	F_0 (eV)	n_0
$2H_2O+H_3O^+$_IS	0.34	−4.58	−95466.88	607
$2H_2O+H_2O$-H_TS	0.44	−4.93	−95466.52	607
$3H_2O$+H*_FS	0.48	−5.15	−95466.60	607
HCOOH+*	0.51	−5.09	−95101.88	600
$HCOO_M$	0.50	−5.50	−95085.50	599
H-COO_M_TS	0.44	−5.21	−95085.31	599
H*+CO_2	0.45	−5.06	−95086.52	599

Supplementary References

1. Qi, Y., Li, J., Zhang, D. & Liu, C. Reexamination of formic acid decomposition on the Pt(111) surface both in the absence and in the presence of water, from periodic DFT calculations. Catal. Sci. Technol., **5**, 3322-3332 (2015).

2. Svane, K.L., Reda, M., Vegge, T. & Hansen, H.A. Improving the Activity of $M-N_4$ Catalysts for the Oxygen Reduction Reaction by Electrolyte Adsorption. *ChemSusChem* **12**, 5133-5141 (2019).

3. Le, J.B. & Cheng, J. Modeling electrochemical interfaces from ab initio molecular dynamics: water adsorption on metal surfaces at potential of zero charge. *Curr. Opin. Electroche.* **19**, 129-136 (2020).

4. E. Yan, R. Balgley, M. B. Morla, S. Kwon, C. B. Musgrave, B. S. Brunschwig, W. A. Goddard and N. S. Lewis, *ACS Appl. Mater. Interfaces*, **14**, 9744-9753 (2022).

5. M. D. Hossain, Y. Huang, T. H. Yu, W. A. Goddard Iii and Z. Luo, *Nat. Commun.*, **11**, 2256 (2020).

6. Y. Huang, R. J. Nielsen and W. A. Goddard, *J. Am. Chem. Soc.*, **140**, 16773-16782 (2018).